

**GEOHERMAL POTENTIAL OF THE
NORTHERN HASSAYAMPA PLAIN,
PART II**

by

Claudia Stone

With a section on Segmentation in Basin-Range Faults by

Christopher M. Menges

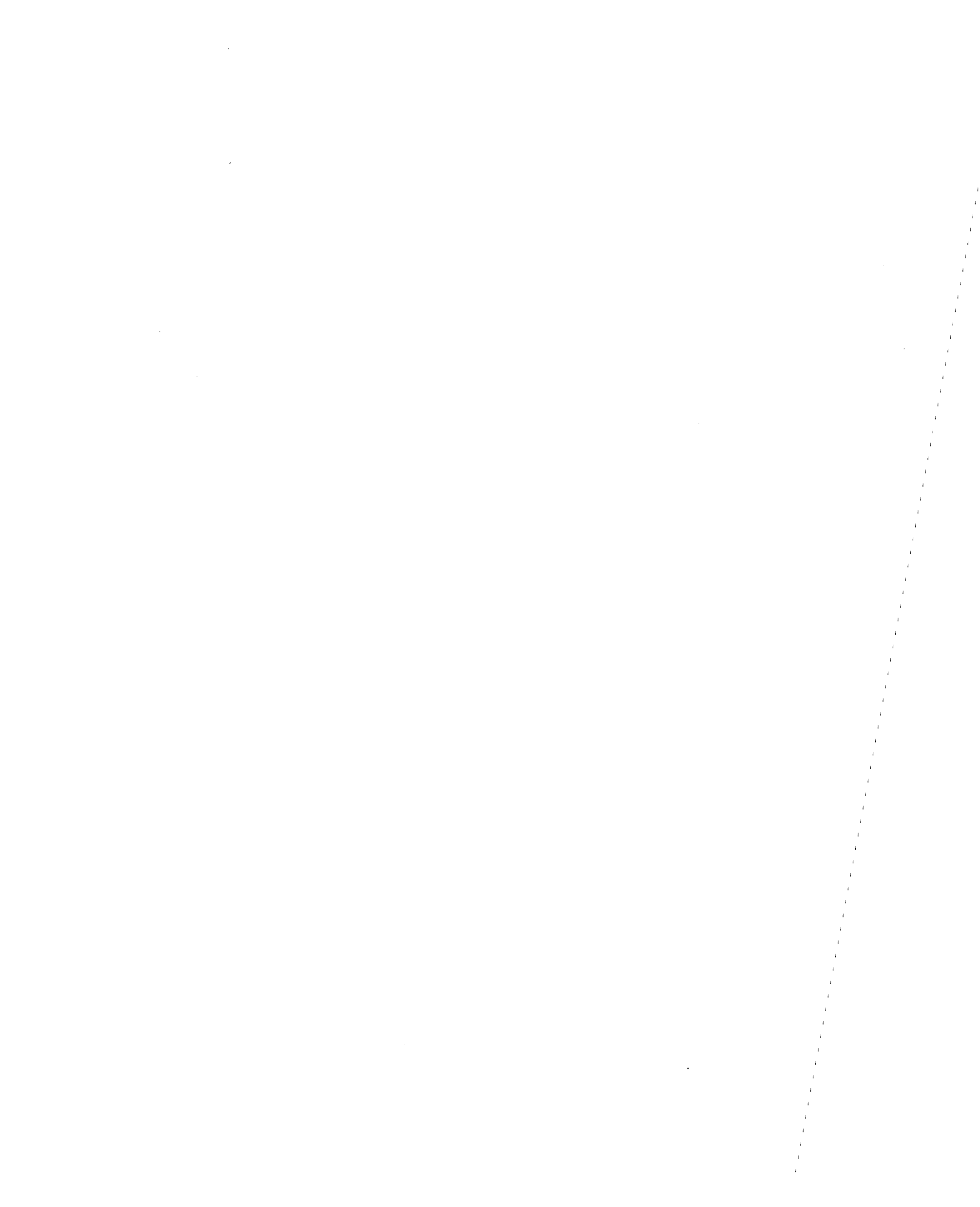
Arizona Geological Survey
Open-File Report 81-25

June 1982

Arizona Geological Survey
416 W. Congress, Suite #100, Tucson, Arizona 85701

*Funded by the U.S. Department of Energy
Contract Number DE-FC07-79ID12009*

This report is preliminary and has not been edited
or reviewed for conformity with Arizona Geological Survey standards



GEOHERMAL POTENTIAL OF THE NORTHERN
HASSAYAMPA PLAIN, PART II

Introduction. Stone (1979) reported the occurrence of 53°C water in a well on the northern Hassayampa Plain. On the basis of water and soil geochemical surveys and a thermal gradient survey she postulated that the warm water is rising at the intersection of a northwest-trending range-bounding fault and a northeast (?) -trending basement fault. Exploration work in the northern Hassayampa Plain was continued during FY-80 in an attempt to further define the geothermal anomaly that exists there and to provide some information on its structural setting. The more recent work include: (1) reconnaissance geologic mapping; (2) collecting ground-water and additional mercury-soil samples; and (3) a gravity survey.

Geology. The Belmont Mountains are a small, northwest-trending mountain range located in west-central Arizona about 72 km northwest of Phoenix (Fig. 1). The range and the unnamed volcanic and metamorphic rocks at the northwest end of the range form the southern boundary of the northern Hassayampa Plain. The Vulture Mountains form the northern boundary.

Previous mapping in the Belmont Mountains includes the Geologic Map of Maricopa County, scale 1:375,000 (Wilson, Moore, and Peirce, 1957) and the Geologic Map of Arizona, scale 1:500,000 (Wilson, Moore, and Cooper, 1969), both of which indicate that the range is underlain by Precambrian granite with Tertiary-Cretaceous intrusive rocks at the south-east end. Mapping by Fugro, Inc., (personal commun., 1979) completed only along the southwest side of the range, indicated that the main part of the mountain is underlain by granite, with the southeast quarter of the range being "fine grained andesite." A regional reconnaissance geologic map by Reynolds (1980) shows rock types similar to those on the state and county maps, but includes a

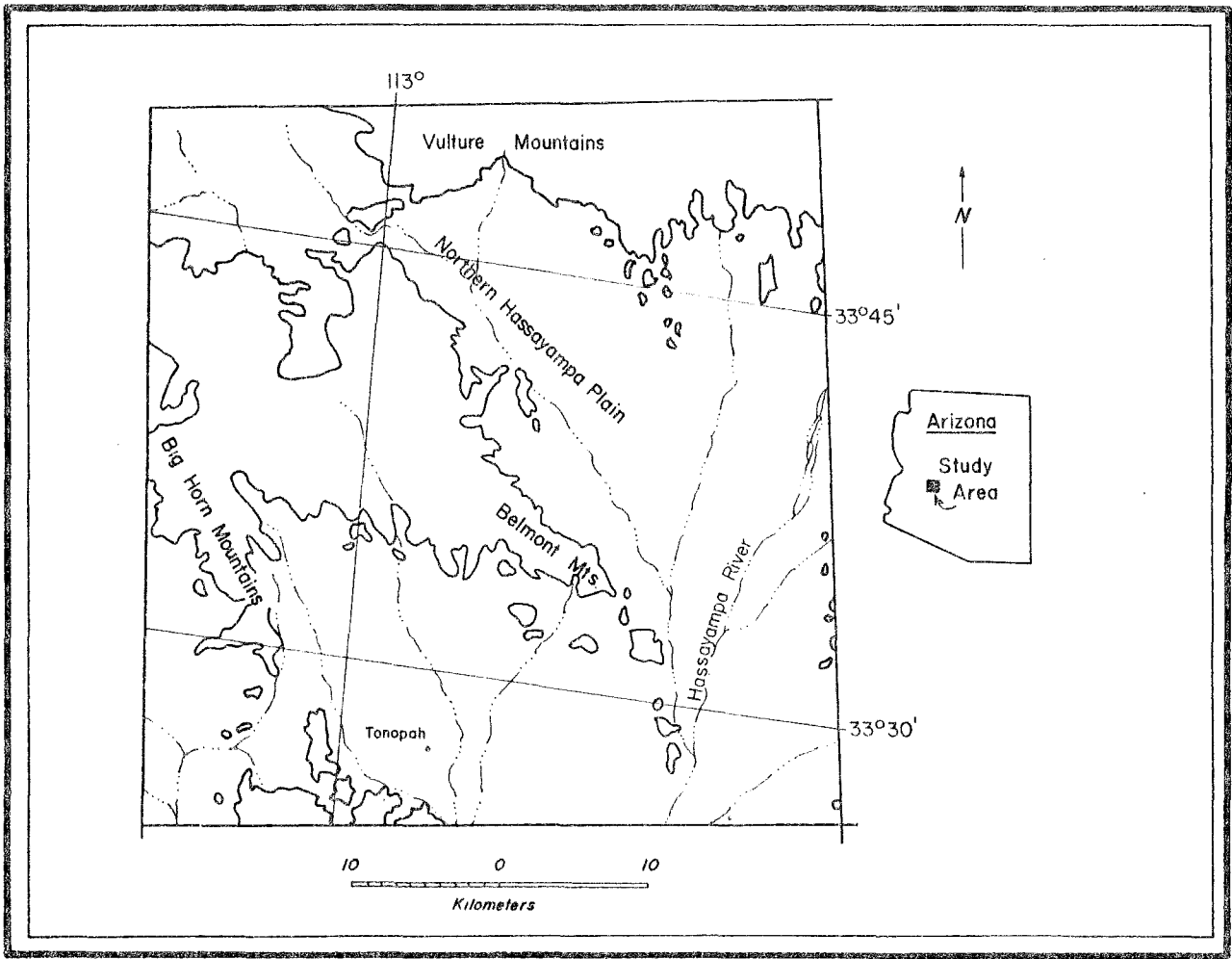


Figure 1. Location map, northern (and southern) Hassayampa Plain, Arizona

small area of metamorphic rock in the southeastern part of the mountain.

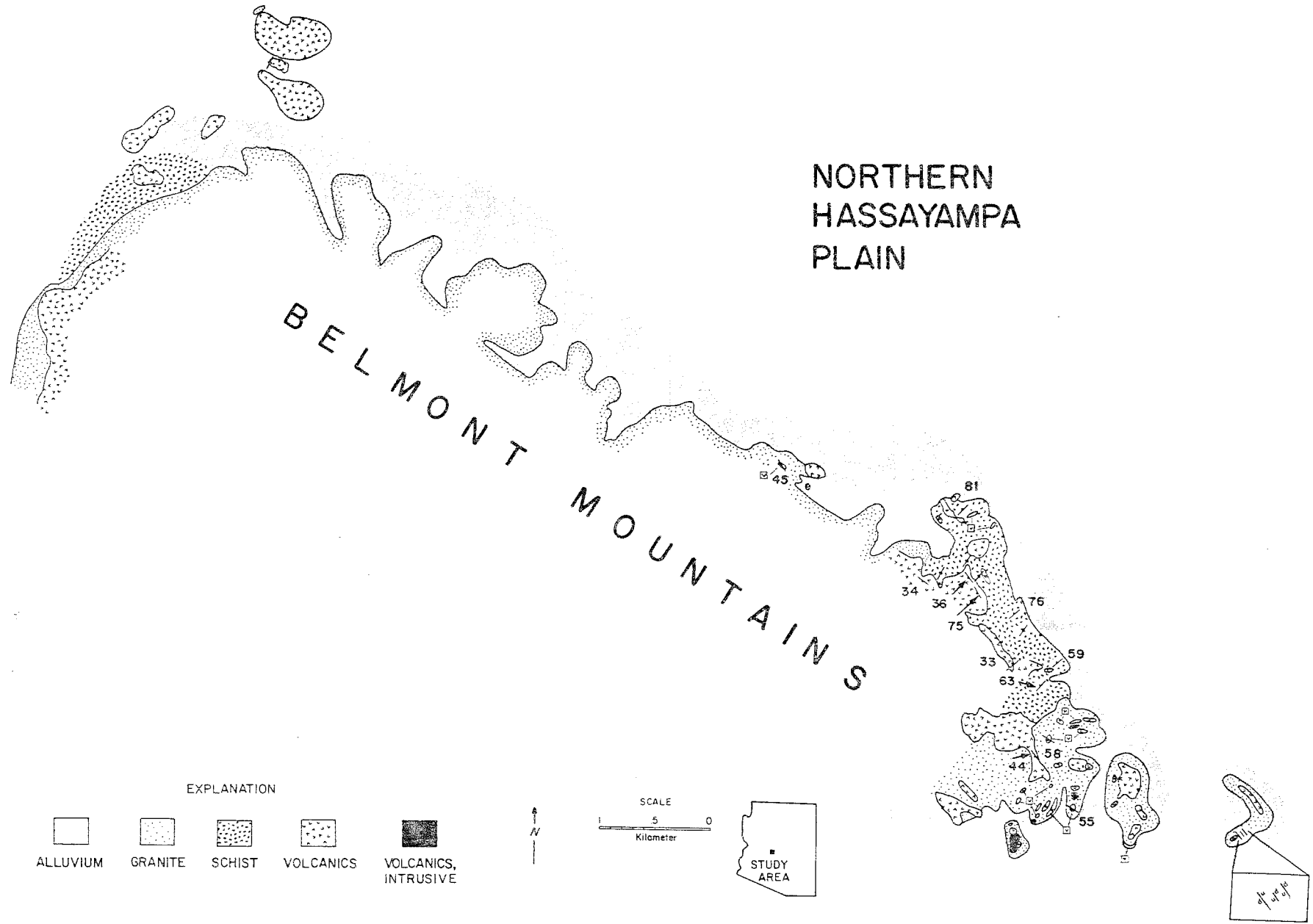
The purpose of this mapping project was to confirm existing geologic work and to improve detail by enlarging the map scale to 1:24,000. In addition we were looking for evidence in the range block of large-scale north-east striking fault (s) that might reasonably be interpreted to project into the basement rocks underlying the basin. Such a fault would intersect the northwest-trending master fault. We postulated that the basement geometry resulting from differential movement along intersecting faults could provide the structural control that is responsible for the rising thermal water. The two weeks of field time allotted for this work were insufficient to complete the mapping project because much of the previous work was not accurate.

Our reconnaissance geologic mapping (Fig. 2) revealed that the southeast end of the Belmont Mountains is comprised predominantly of Precambrian (?) granitic and metamorphic rocks, with minor diabasic plugs and dikes. The crystalline rocks have been intruded by rhyolitic to andesitic dikes and sills of probably mid-Tertiary age.

The metamorphic rocks at the southeast end of the Belmont Mountains grade from phyllite to schist to minor gneiss and amphibolite, with schist predominating. The schists vary in color from pale to very dark green and in texture from massive to schistose. Foliation strikes northeast, generally N. 37 to 48°E. Dips are steep and increase northwestward to nearly vertical. Referring to similar features found in the Vulture Mountains to the north, Rehrig, Shafiqullah, and Damon (1980, p. 92) stated that such "structural attitudes are similar to those in Precambrian terranes elsewhere in Arizona and are probably the result of Precambrian deformation."

The Precambrian (?) granitic rocks that invaded the metamorphic rocks represent several episodes of emplacement. However, the Precambrian age of

Figure 2. Generalized geology, Belmont Mountains



these granites may be somewhat questionable because 68.4 m.y. old granitic rocks in the Vulture Mountains were considered to be Precambrian prior to radiometric age dating (Rehrig and others, 1980). The granitic rocks of the southeast Belmont Mountains generally have a fine-grained subhedral texture, with minor (<1%) to moderate (10%) amounts of mafic minerals--principally biotite. Locally some granitic rocks have a very fresh appearance; others are quite weathered, with biotite altering to chlorite (?). At one locality the rocks contain both biotite and secondary (?) white mica. Both metamorphic and granitic rocks were intruded by small diabase dikes and plugs.

During the mid-Tertiary, the southeastern end of the range was extensively invaded by andesitic to rhyolitic intrusions (dikes and sills ?). The intrusive rocks are generally porphyritic with varying percentages of feldspar, or quartz and feldspar phenocrysts. Colors range from light gray to pinkish and lavender. These hypabyssal (?) intrusions strike mostly northwest, from N. 31 to 67° W., and dip up to 75° SW. Locally some volcanic rocks contain sparse, weathered mafic (basaltic ?) xenoliths as large as 6 x 9 cm. Two small outcrops of flat-lying basalt were noted at or near the tops of low hills.

Rehrig and others (1980) postulated that the "Big Horn Mountains," a name they used to include the Belmont Mountains, comprise a regional antiform with a northwest-striking axis. They showed that structures southwest of the antiformal axis dip to the southwest and structures northeast of the axis, including the Belmont Mountains, dip to the northeast (Rehrig and others, 1980, Fig. 7). Our mapping in the Belmont Mountains shows that these rocks dip southwest.

Ground-water chemistry. Prior to 1977, only two water chemical analyses from the northern Hassayampa Plain were listed in the U.S. Geological Survey

water quality file. In 1977-78, members of the U.S.G.S. sampled eight wells in the area, but complete analyses were run on only three of the samples (Sanger and Appel, 1980). The remaining five samples were filed analysed only for fluoride and specific conductance. During FY-79 we sampled four wells, which brought to nine the total number of complete chemical analyses available.

It was our intention during FY-80 to sample the five wells that were not analysed by the U.S.G.S. and all other wells we could find. However, discussions with area residents revealed that additional water wells do not exist in this region except for a domestic well recently drilled at the Jones Ranch, NE SE SW sec. 35. T. 6 N., R. 6 W., which is somewhat north of the study area. Apparently, when the range is used for grazing, ranchers truck in water for the livestock, so that most wells have fallen into disrepair and have been abandoned. The five water samples that were collected, but not fully analysed by the U.S.G.S., were taken from standing water in abandon wells and old bore holes. No attempt was made to locate these holes for water samples.

A water sample was collected from the pressure tank on the new well at the Jones Ranch (JR). The major chemical constituents in milligrams per liter (mg/l) are shown, along with those from the Vulture Mine (VM) (sample 9 of Stone, 1979), which is the next closest available water sample, about 1.2 km away. The analyses are not similar. The single largest difference occurs in the chlorine concentrations. Because the JR sample was analysed by a lab that principally does rock assays, and was reported as 0.25 gr/l, we suspect there may be an order-of-magnitude error in the reporting. The JR and other Hassayampa samples are also dissimilar, which is not surprising considering the distance between them and the difference in the geology. The JR well is situated on the Vulture Mountain pediment; the other water samples are from

wells drilled in basin-fill sediments.

Geothermometers for the JR water sample (Table 1) show the best correspondence between the Na-K-Ca geothermometer and the cristobalite geothermometer, which was true with the VM water sample and certain of the other Group I water samples (see Stone, 1979). The JR correlation is poor, but it does indicate low (35°C) subsurface temperatures in this area, as predicted by the VM geothermometers (Table 1).

Table 1. Chemical analyses in milligrams per liter of ground water from the Jones Ranch and the Vulture Mine

<u>Constituent</u>	<u>JR</u>	<u>VM</u>
pH	7.8	7.7
Na	37.0	77
K	2.0	1.6
Ca	52.0	25.0
F	2.1	3.2
Cl	250.0	27.0
SO ₄	70.0	19.0
HCO ₃	270.0	250.0
SiO ₂	47.0	23.0
TDS	365.0	309.9
Mg	*	10.0
^T SiO ₂	48.6°C	36.9
^T Na-K-Ca	23.7	36.4

*not analysed

Mercury soil survey. A total of 97 mercury soil samples from the northern Hassayampa Plain have been analysed to date (Fig. 3). Of these, 29 were collected during FY-80, in an effort to extend the survey coverage south of master fault boundary and to sample several areas to the north of the fault that were missed during FY-79.

Nearly half of the new analyses (13) exceed 25 ppb Hg, the mean Hg value that was established during the earlier survey. The newer analyses show that anomalous concentrations of mercury occur on both sides of Jack Rabbit Wash, the southeast-trending wash that is inferred to be structurally controlled by the range-bounding fault along the Belmont Mountains. More important, the more recent analyses clearly highlight the northwest fault that was indentified during the preliminary study (Stone, 1979). The northeast-trending fault suggested in the earlier study is less conspicuous. A large concentration of anomalously high mercury values clusters around the 53^oC thermal well. A group of low values clusters in the central basin area.

Gravity. A gravity survey was conducted over the western part of the northern Hassayampa Plain. Prior to this survey, gravity data were scarce in this region. A single township to the east was surveyed in 1973 by Fugro, Inc., who kindly allowed us to use their data in this report.

Elevations and lat/lon control for our survey were obtained from the U.S. Geological Survey, Topographic Division, Menlo Park; through leveling; or were extrapolated from the Vulture Mountains and Belmont Mountains 15' topographic quadrangle maps. Reduction and correction of all data and gravity modeling were accomplished by computer in the laboratory of Dr. Carlos L.V. Aiken, University of Texas at Dallas. Density contrast was determined by measurements on actual drill core from the western part of the Hassayampa Plain (drillhole #1). The gravity data were contoured at 2-milligal intervals (Fig. 4).

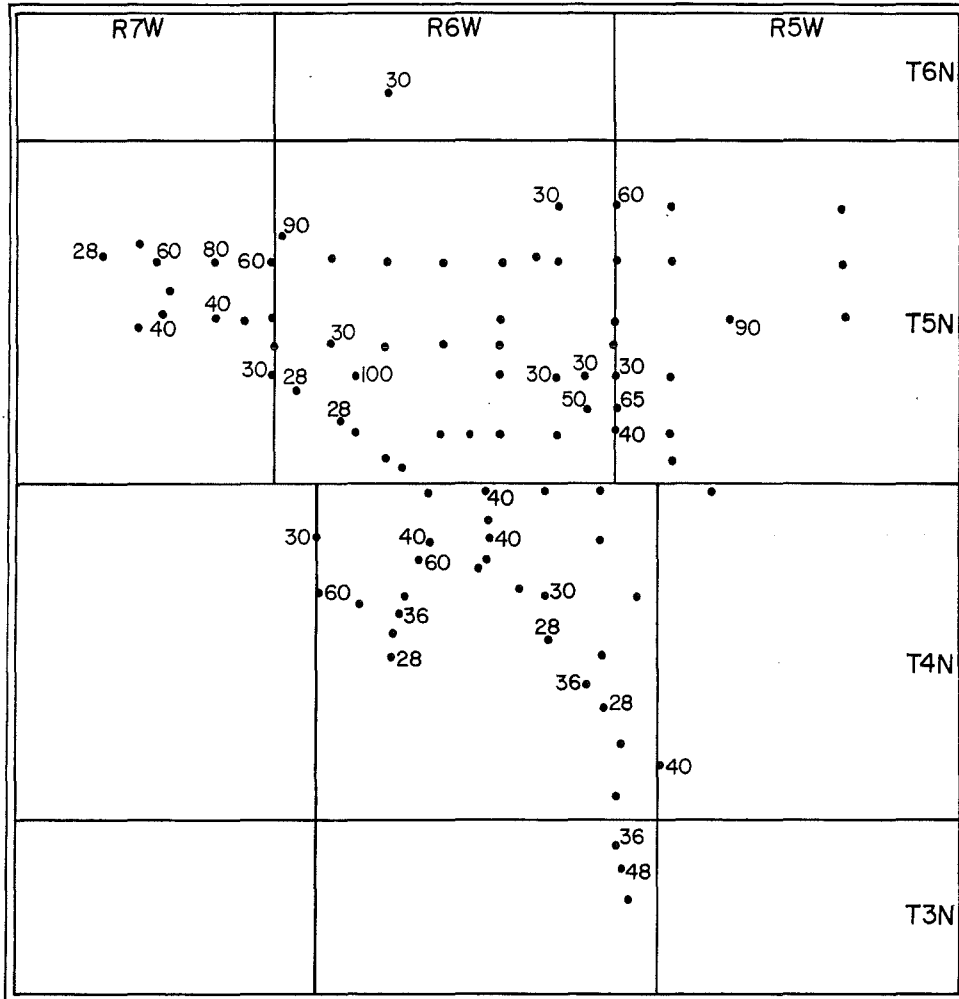


Figure 3. Location of samples collected for mercury-soil survey. Numbers are mercury contents in ppb for samples having concentrations greater than 25 ppb.

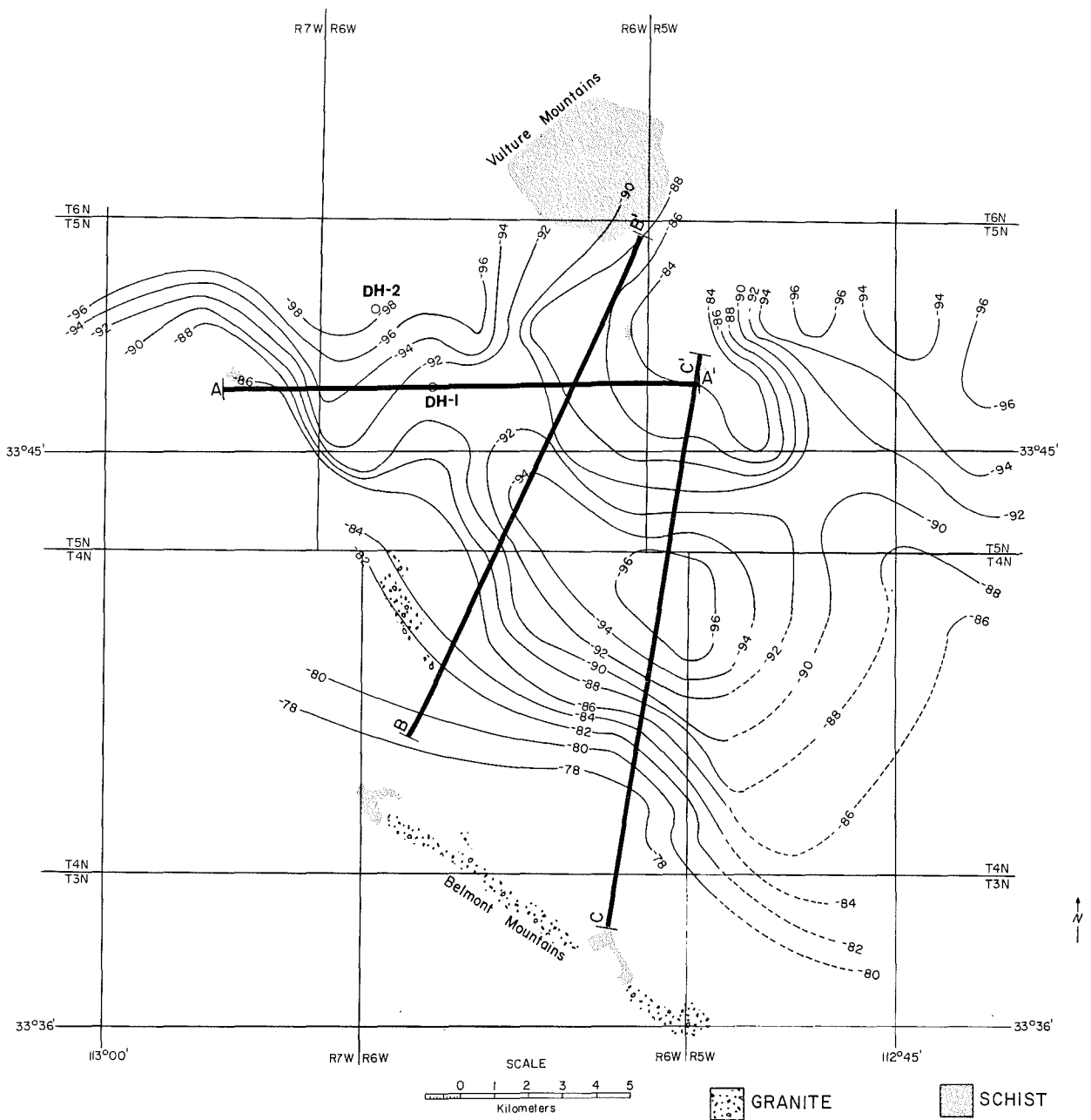


Figure 4. Gravity map of the northern Hassayampa Plain, with profiles used for two-dimensional modeling (Fig. 5a-c). Contour interval is 2 milligals.

Two structural features are readily apparent from the gravity map. First, the northwest-trending pediment edge of the Belmont Mountains is a sinuous rather than a linear feature. The sinuosity suggests that the master fault boundary is segmented, a feature recognized by Menges (1981) in the Sonoita Creek basin (see Appendix). Second, complex faulting in the basement has occurred with probable rotation of basement blocks. As a result of such faulting and rotation it is likely that the basement blocks are highly fractured. Mostly probably though the fractures were later sealed by secondary mineralization and dike intrusions. Highly faulted and fractured schistose rocks that crop out in the Vulture Mountains to the north have been intruded by numerous such veins and dikes.

Three profiles were picked for 2-dimensional modeling (Fig. 4), using the Backus-Gilbert inversion method. Interpretative structural cross sections were constructed from these profiles (Fig. 5). The gravity map and the cross sections clearly show that the deepest part of the basin occurs beneath sec 1, T. 4 N., R. 6 W. The basin is a relatively narrow, fault-bounded graben that is deepest (about 1,250 m) at the southeast end (Figs. 4 and 5C; Profile C-C'). Bedrock shallows to the northwest to about 730 m (Figs. 4 and 5B; Profile B-B). A horst block (erosional bedrock high?) separates the main graben from what is probably an equally deep fault-bounded basin to the northwest. Drill Hole No. 1 (DH-1) located over the horst block, encountered schist at a depth of 332 m. Drill Hole No. 2 (DH-2), which is about 30.5 m higher in elevation than DH-1, did not get out of basin fill at a total depth of 383 m. Another horst block or bedrock high(?) can be seen north of the deepest basin, about where profiles A-A' and C-C' intersect. Low hills of schist crop out in this area.

Gravity data are scarce in the southeast corner of the study area.

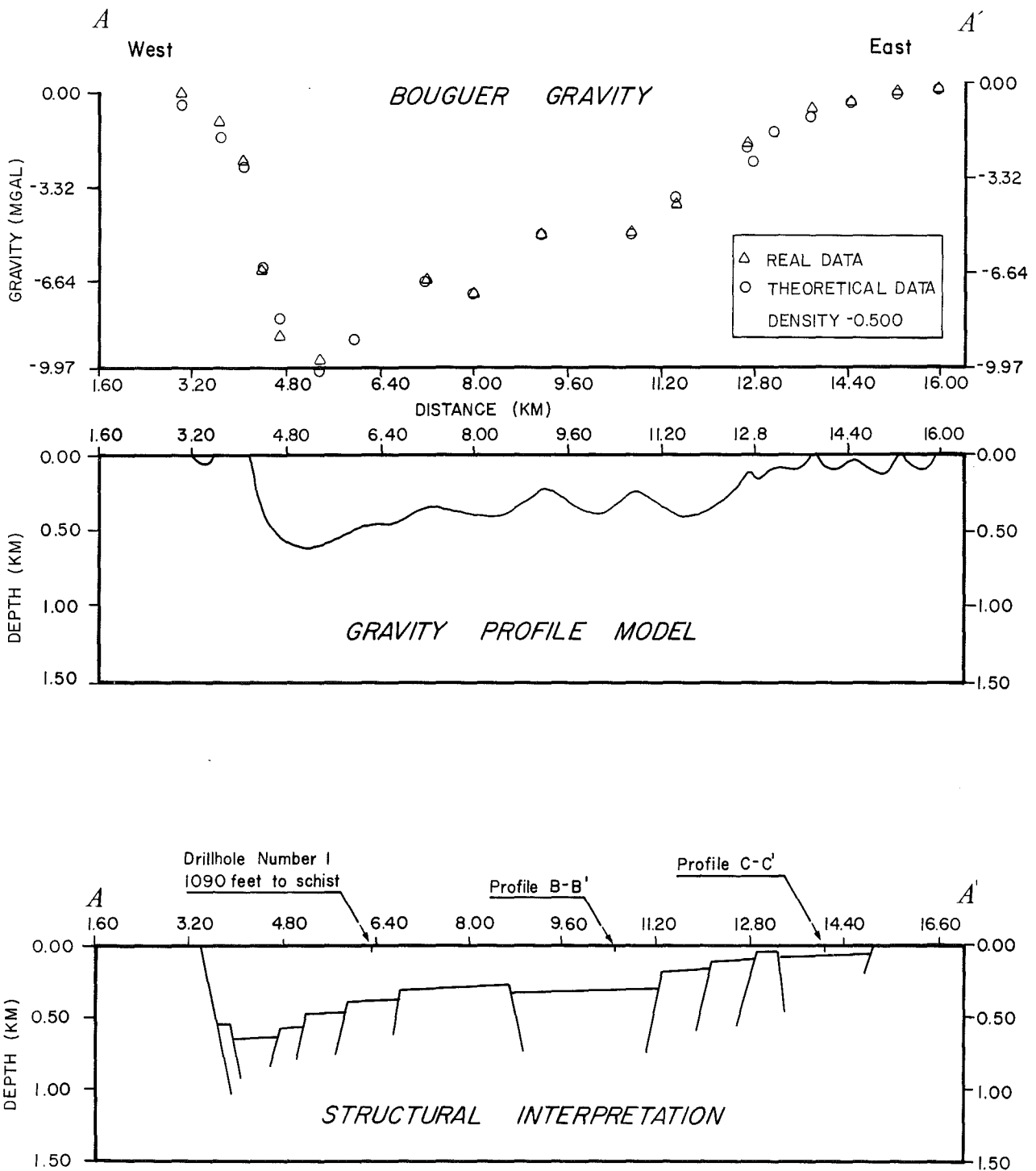


Figure 5a. Two-dimensional gravity profiles and interpretative structural cross sections.

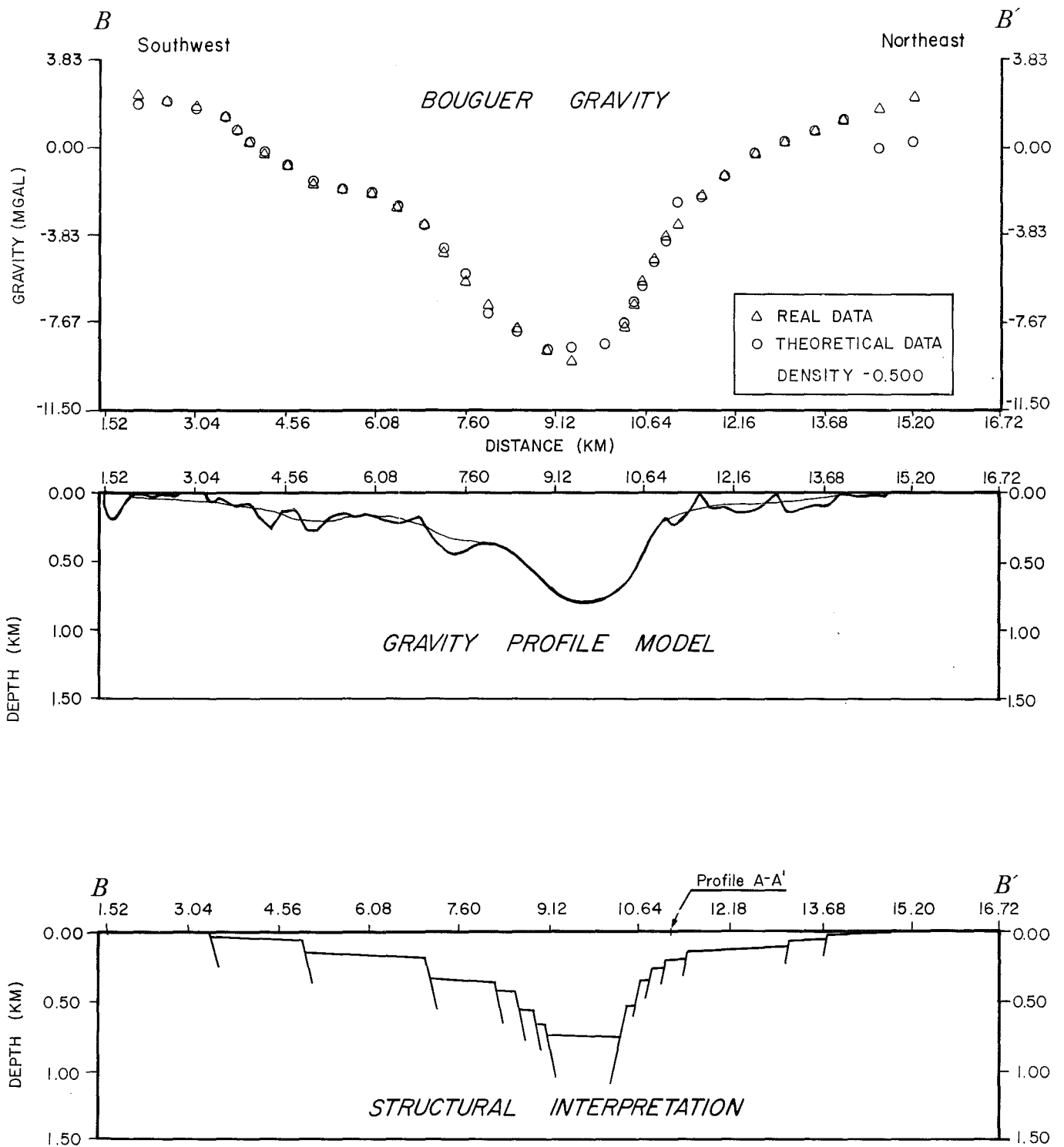


Figure 5b. Two-dimensional gravity profiles and interpretative structural cross sections.

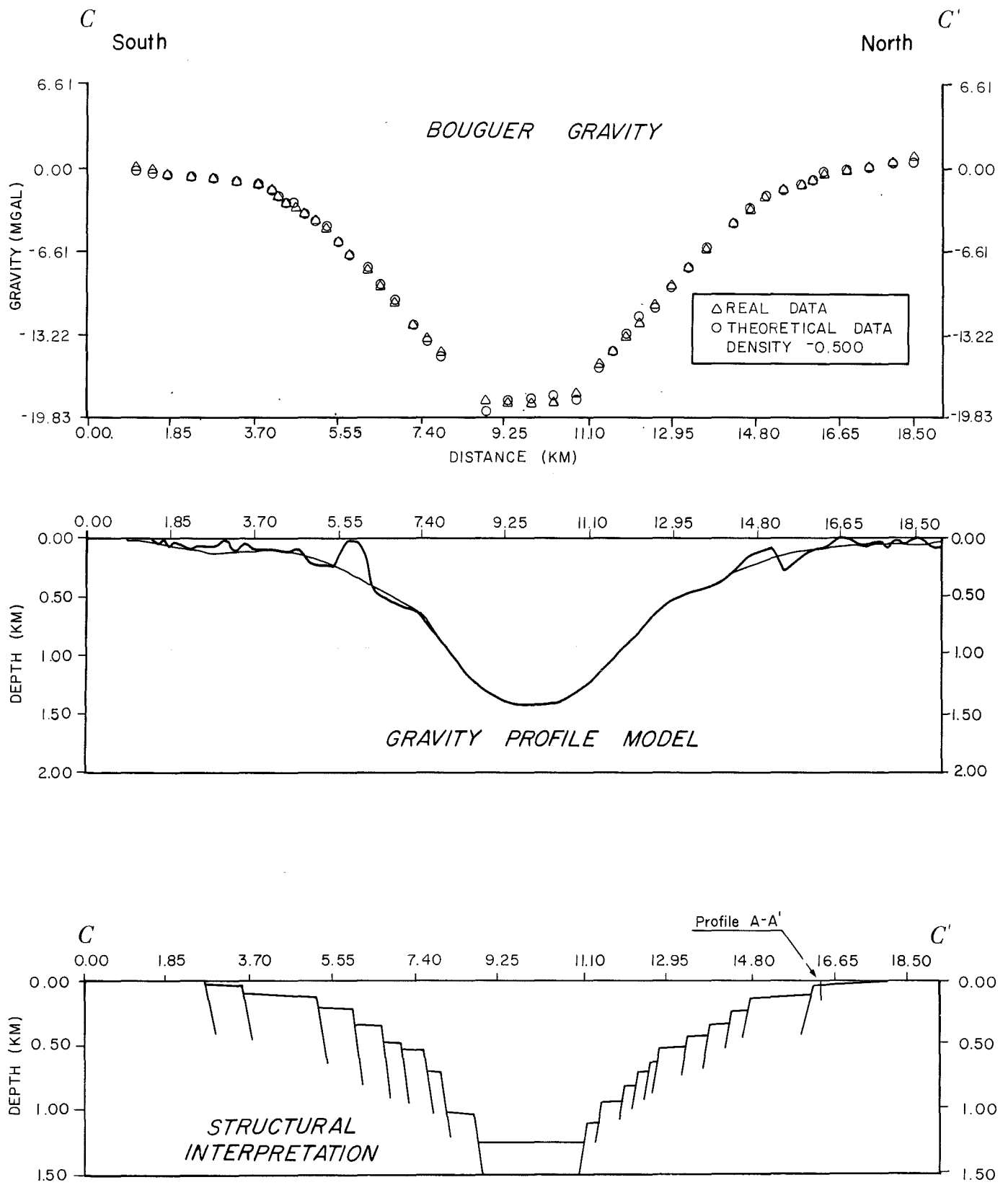


Figure 5c. Two-dimensional gravity profiles and interpretative structural cross sections.

However, the gravity contours appear to be influenced by the pediment of the White Tank Mountains.

Traces of fault zones have been interpreted based on the gravity data and modeling, and are shown in Figure 6 .

Isotherms. Four cross sections showing subsurface temperature distributions (Fig. 7) were constructed from well temperatures measured in FY-79 (Stone, 1979, Fig. 11). The profiles show that warm water is ascending in the area of well A, and to a lesser extent, wells B and C. In profile A-A', the isotherms are nearer the surface in well B, which is located within the major fault zone (Fig. 6). Isotherms in profile B-B' show that warm water is also rising in the area of well A and that the fluids are confined to a narrow zone. Wells D and J appear to be unaffected. Well A is located within the fault zone that comprises the northeast graben boundary. It can be seen in profile C-C' that wells E, F, and G are not involved in the thermal system. Profile D-D' again shows that warm water ascends principally in the areas of wells A and B.

The cross sections suggest that the northeast and southwest graben-bounding faults, or discreet segments of them, are conduits for rising warm water. The conduits most likely occur where vertical permeability is sufficiently great to allow fluid flow.

If warm water is rising in the area of well C, which is inferred from the temperature-depth profile of that well (Stone, 1979, Fig. 11), the explanation for this anomaly is quite different. Well C, which is also DH-1, sits atop a horst block. We suggest that normal ground water, moving southeast from the next basin, encounters a constriction (see Fig. 5a, Profile A-A'), setting in motion forced ground-water convection. This idea was proposed by Harder and others (1980) and Morgan and Daggett (1981) to explain the primary

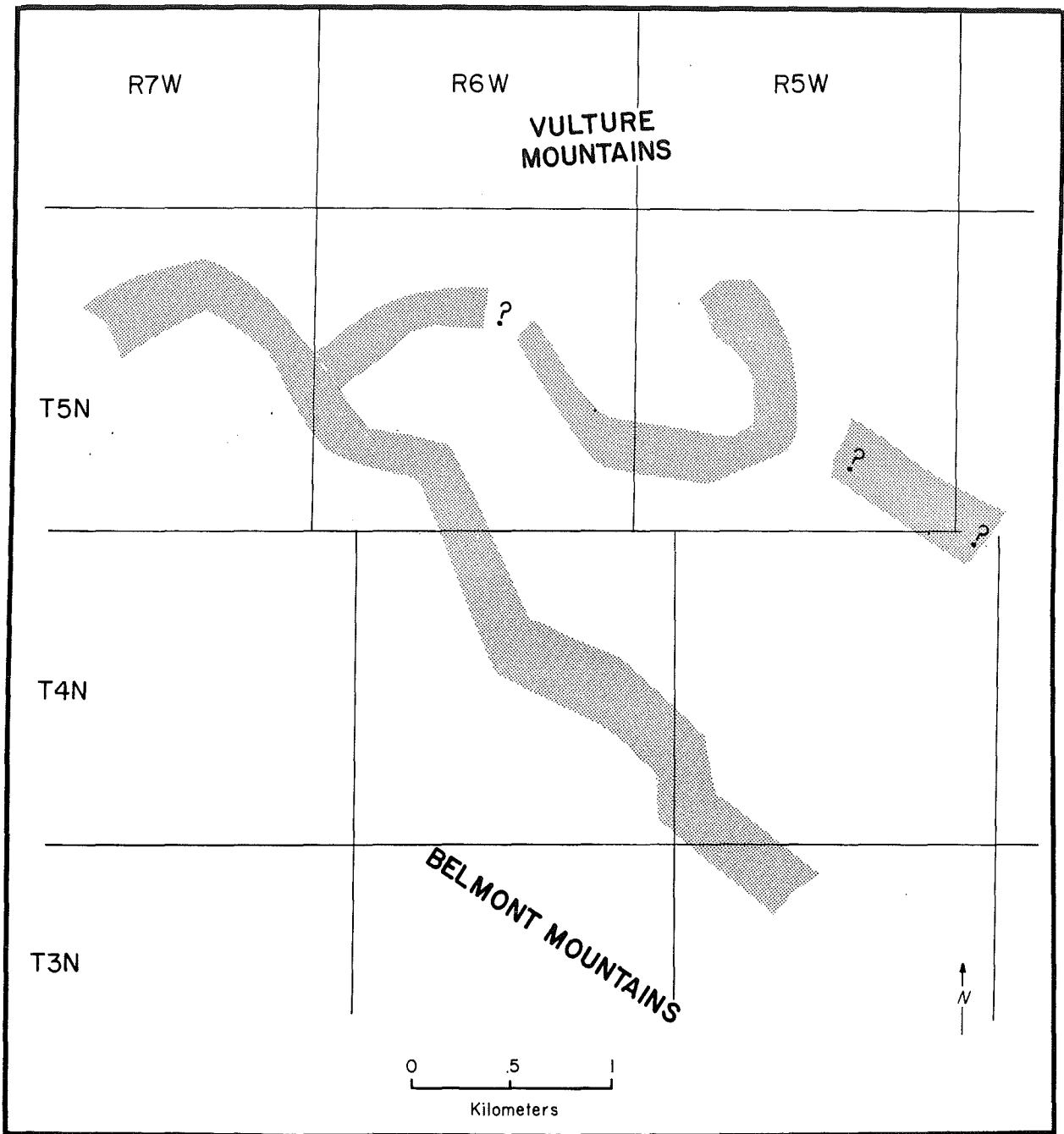
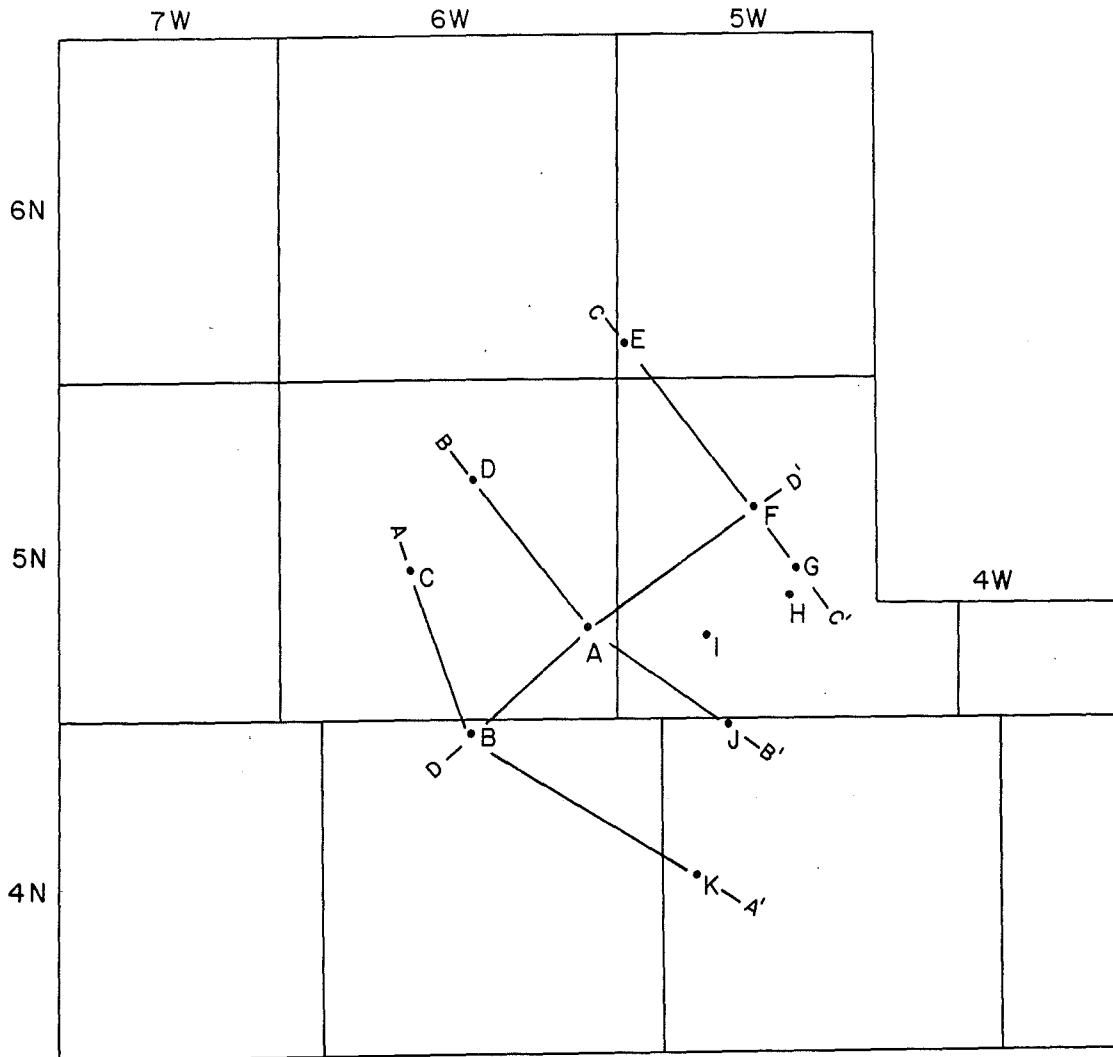


Figure 6. Suggested fault zones based on gravity survey, northern Hassayampa Plain, Arizona

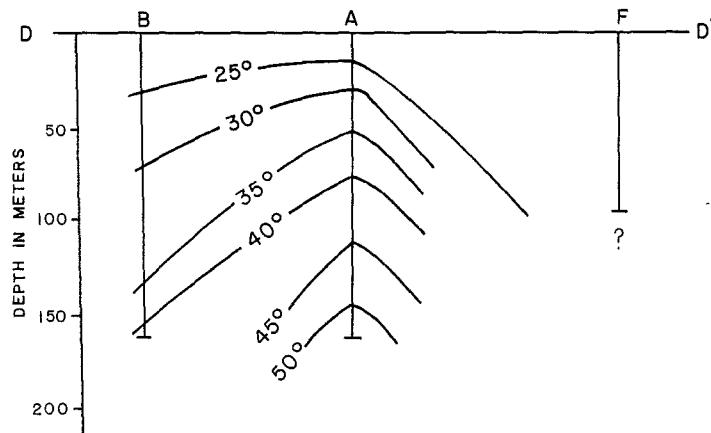
Figure 7. Isothermal cross sections

NORTHERN
HASSAYAMPA
PLAIN, ARIZONA



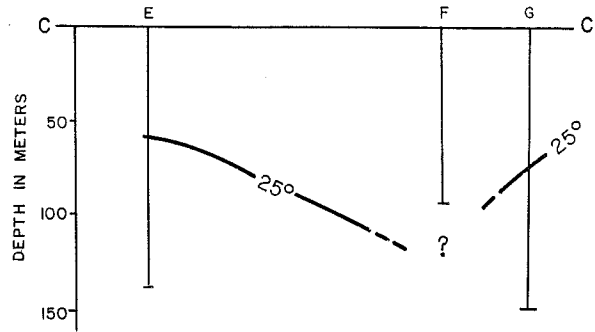
Lines of sections and well locations

Cross section
D-D'

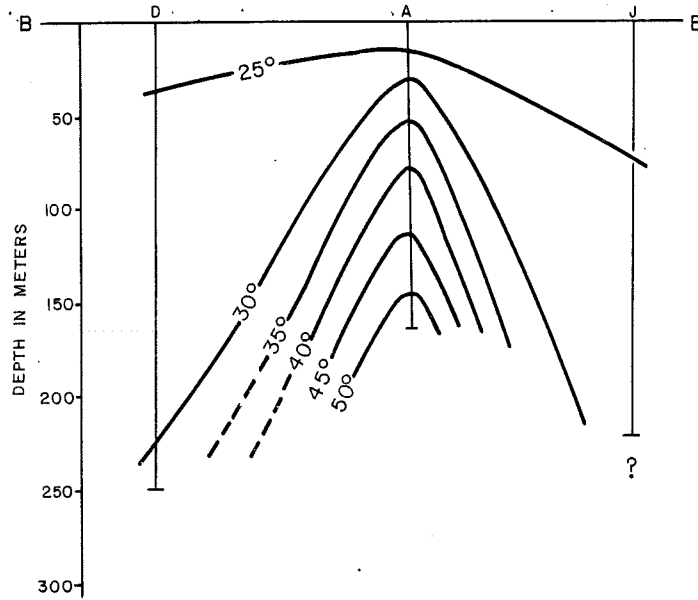


NORTHERN
HASSAYAMPA
PLAIN, ARIZONA

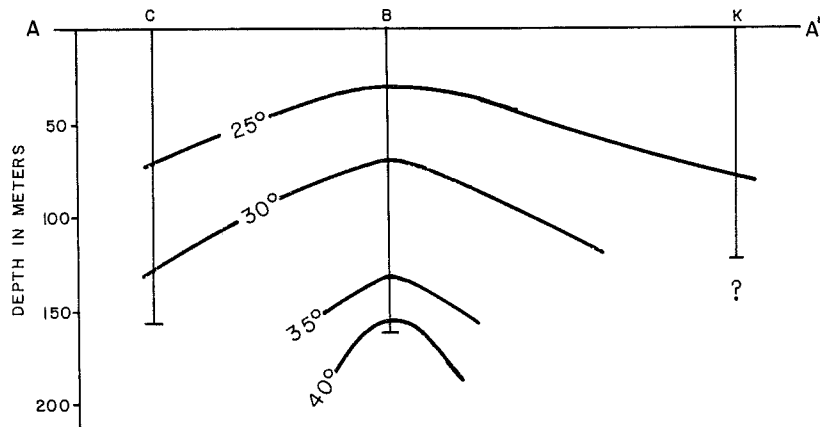
Cross section
C-C'



Cross section
B-B'



Cross section
A-A'



source mechanism for the numerous geothermal anomalies along the Rio Grande rift, New Mexico, excluding the Jemez Mountains. Morgan and others (1981) tested this concept using an analytical model and concluded that "forced groundwater convection is easily capable of causing major gradient anomalies along the rift..." They suggested that "the model may explain many of the geothermal anomalies throughout the Basin and Range province of the western U.S."

Summary and Conclusions. The northern Hassayampa Plain is underlain by a narrow, sediment-filled graben that trends northwest. A gravity survey reveals that the southwest master-fault boundary is segmented and that the basement blocks are faulted and probably rotated. Depths to bedrock range from surface exposures of schist to 1,250 m. Left-stepping asymmetric segmentation of the master fault has been interpreted by Menges (see Appendix) as an expected result of "approximately east-west directed extension...obliquely applied to a northwest-trending fault zone formed and(or) reactivated during the Basin-Range disturbance."

Three geothermal gradients identified in the earlier study as defining a discreet area of hydrologic discharge (Wells A, B, and C; Stone, 1979) are here reinterpreted on the basis of subsurface structures revealed by gravity. Well C is located above a horst block and is now inferred to have a high gradient as a result of forced flow of deep warm water over the horst at the basin hydrologic outlet. Wells A and B are located within the northeast and southwest master fault zones, respectively, and while both reflect zones of rising warm water, they are not obviously related to one another. The warm water is a result of meteoric water circulating to great depths where it is heated in a normal geothermal-gradient regime. Hydraulic head and lower

density then allow the heated fluids to rise toward the surface along the basin-bounding faults.

Two distinct possibilities suggest themselves with respect to disposition of the fluids during or after ascent. First, large volumes of thermal fluids are rising from depth and flowing into a fractured basement beneath the deepest part of the basin. The heat is trapped and stored in a geothermal reservoir in the basement by the overlying, thermally insulating sediments. The alternate possibility is that small volumes of warm water are circulating upward into the overlying sediments where discrete zones of vertical permeability exist in the basement rock. The warm water is carried away or "washed out" by the down-gradient flow of shallow cold ground water in the basin-fill sediments.

The first possibility, the existence of a significant geothermal reservoir in the basement, is unlikely for several reasons. There is no evidence for a large heat anomaly in this region. Tectonic activity and volcanism in the Vulture Mountains ceased more than 10 million years ago (Rehrig, Shafiquallah, and Damon, 1980) and by correlation, the Belmont Mountains have been inactive at least that long. Anomalous concentrations of radioactive elements are not known to exist in the crystalline or sedimentary rocks in this area (Scarborough and Wilt, 1979; Malan and Sterling, 1969). A single heat flow measurement in the Vulture Mountains has only a moderate value for the Basin and Range province (J. Sass, personal commun., 1979). The final argument is that both measured and predicted temperatures for this area can be achieved in a normal Basin-and-Range heat-flow regime. Using a mean annual air temperature of 20°C and a normal gradient of 30°C/km, a temperature of 57.5°C would be expected at 1,250 m depth. In addition, meteoric water need circulate to depths of only about 2.0 km in a normal-gradient region to achieve the 73°C temperature predicted by the chemical geothermo-

meters (Stone, 1979). Such circulation depths are believed easily reached in a normal Basin-and-Range structural setting. I infer from the above information that meteoric water circulates through at least the upper 1,000 m of basement in this basin, but that a geothermal reservoir does not exist in the basement.

Additional lines of evidence support the second explanation. Specifically, geothermal gradients were measured in 11 wells in this area, ten of which are located above the master fault zones. Of the 11 wells, two have gradients that are about normal (23 and 25°C/km); five gradients are greater than 40°C/km, and four are below normal (19 to 9°C/km). Wells with above-normal gradients exist within 2 or 3 km of wells having below-normal gradients. This proximity of high and low-gradient wells to one another, nearly all of which are above the fault zones, strongly suggests that the upward flow of warm water is a very localized phenomenon. Wells A and B obviously intercept warm water circulating upward into the overlying sediments, but these two wells overlie two separate and distinct fault zones and are not related.

Electrical studies such as resistivity or Schlumberger soundings, shallow (3 m) temperature-gradients survey over the deep basin, and deep gradient or heat flow holes (~1,000 m) might provide sufficient additional information to reverse the present conclusions.

Deep drilling in the area of Well A (and perhaps Well B) probably would encounter thermal waters with temperatures at least to 70-75°C, but the occurrence of such fluids most likely would be localized and volumes would be relatively small. Sufficient volumes and temperatures may exist for small-scale, low-temperature direct uses.

REFERENCES

- Harder, V., Morgan, P., and Swanberg, C.A., 1980, Geothermal resources of the Rio Grande rift: Origins and potential: Geothermal Resources Council Transactions, v. 4, p. 61-64.
- Malon R.C., and Sterling, D.A., 1969, A geological study of uranium resources in Precambrian rocks of the western United States: U.S. Atomic Energy Commission Report AEL-RD-9, January 1969, Grand Junction, Colorado office, 54 p.
- Morgan, P., and Daggett, P.H., 1981, Active and passive seismic studies of geothermal resources in New Mexico and investigations of earthquake hazards to geothermal development: New Mexico Energy Research and Development Program, Technical Compilation Report EMD 77-2203, Los Cruces, N.M., 50 p.
- Morgan P., Harder, V., Swanberg, C.A., and Daggett, P.H., 1981, A groundwater convection model for Rio Grande rift geothermal resources: Geothermal Resources Council Transactions, v. 5, p. 193-196.
- Rehrig, W., Shafiqullah, M., and Damon, P., 1980, Geochronology, geology and listric normal faulting of the Vulture Mountains, Maricopa County Arizona: Arizona Geological Society Digest, v. 12, p. 89-110.
- Reynolds, S.R., 1980, Geologic framework of west-central Arizona: Arizona Geological Society Digest, v. 12, p. 1-16.
- Sanger, H.W., and Appel, C.L., 1980, Maps showing ground-water conditions in the Hassayampa area, Maricopa and Yavapai Counties, Arizona - 1978: U.S. Geological Survey Water-Resources Investigations Open-File Report 80-584.
- Scarborough, R.B, and Wilt, J.C., 1979, A study of uranium favorability of Cenozoic sedimentary rocks, Basin and Range province, Arizona: U.S. Geological Survey Open-File Report 79-1429, 101 p.
- Stone, C., 1979, Preliminary assessment of the geothermal potential of the northern Hassayampa Plain, Maricopa County, Arizona: State of Arizona, Bureau of Geology and Mineral Technology Open-File Report 79-17, 42 p.
- Wilson, E.D., Moore, R.T., and Cooper, J.R., 1969, Geologic map of Arizona, Scale 1:500,000, The Arizona Bureau of Mines.
- Wilson, E.D., Moore, R.T., and Peirce, H.W., 1957, Geologic Map of Maricopa County, scale 1:375,000, The Arizona Bureau of Mines.

APPENDIX TO GEOTHERMAL POTENTIAL OF THE
NORTHERN HASSAYAMPA PLAIN, PART II

Segmentation In Basin-Range Faults

Christopher M. Menges

A detailed gravity survey of the northern Hassayampa Plain conducted by Claudia Stone (this report) indicates a well-defined northwest-trending residual gravity low centered over the alluvial basin (Fig. 4, this report). A steeply sloping and sinuous gravity gradient forms the southwest boundary of the anomaly. Quantitative 2-dimensional modeling across this portion of the gravity anomaly by C.L.V. Aiken demonstrates that the boundary represents a steeply dipping fault zone bounding a northwest-oriented, complex asymmetric graben (Fig. 4, this report). Further, the sinuous trace of the anomaly gradient suggests that this master fault boundary is segmented; that is, it varies abruptly in strike, so as to define a repetitive sequence of alternating west-northwest and north-northwest-trending segments, which fluctuate about the average northwest orientation of the composite fault zone.

This pattern closely resembles the geometries of Basin-Range structures defined by detailed gravity surveys and structural mapping and analysis in Sonoita Creek basin (Menges, 1981), a 100 km² alluvial valley located 60 km southeast of Tucson in southeastern Arizona. Similar 2-dimensional modeling of the Sonoita Creek basin-centered residual gravity low has revealed a complex asymmetric graben bounded to the southeast by a very steeply dipping master fault boundary (Fig. A-1). In plan, the Sonoita Creek graben itself abruptly deflects from northeast to north-northwest and north-south orientations across the length of the basin thereby outlining a grossly kinked segmented pattern. Also, several structural boundaries to the graben display segmentation geometries (Fig. A-2; e.g., the west, southeast and northeast

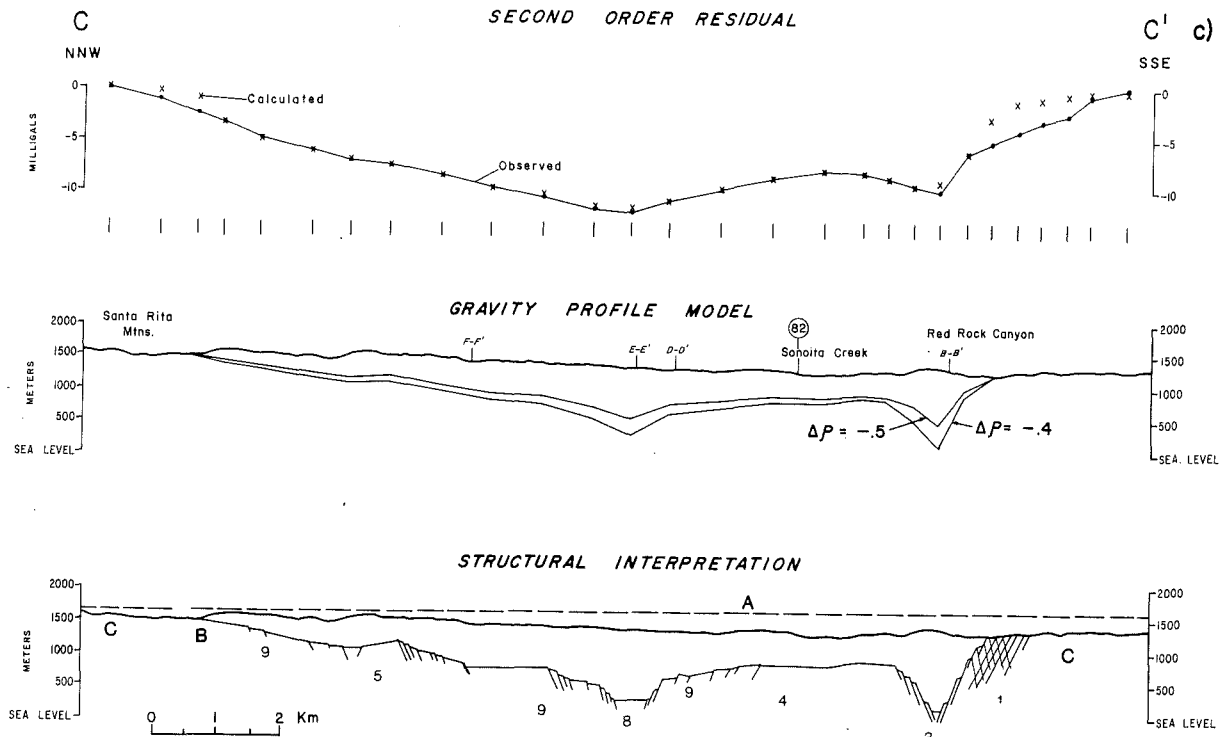


Figure A-1. One of six Two-dimensional Profile Models across the residual gravity anomaly of Sonoita Creek Basin. -- Refer to Fig. 2 for profile locations. Each model includes: (a) observed and calculated residual anomaly values for each model prism center (upper profile); (b) two bedrock depth profiles calculated at each prism center, using density contrasts of $\Delta\rho = -0.4$ and -0.5 g/cm^3 (middle profile); and (c) an interpretative subsurface structural cross section, based on the calculated bedrock depth profile ($\Delta\rho = -0.4 \text{ g/cm}^3$) combined with surface structural data (lower profile). No vertical exaggeration is present in the depth profile.

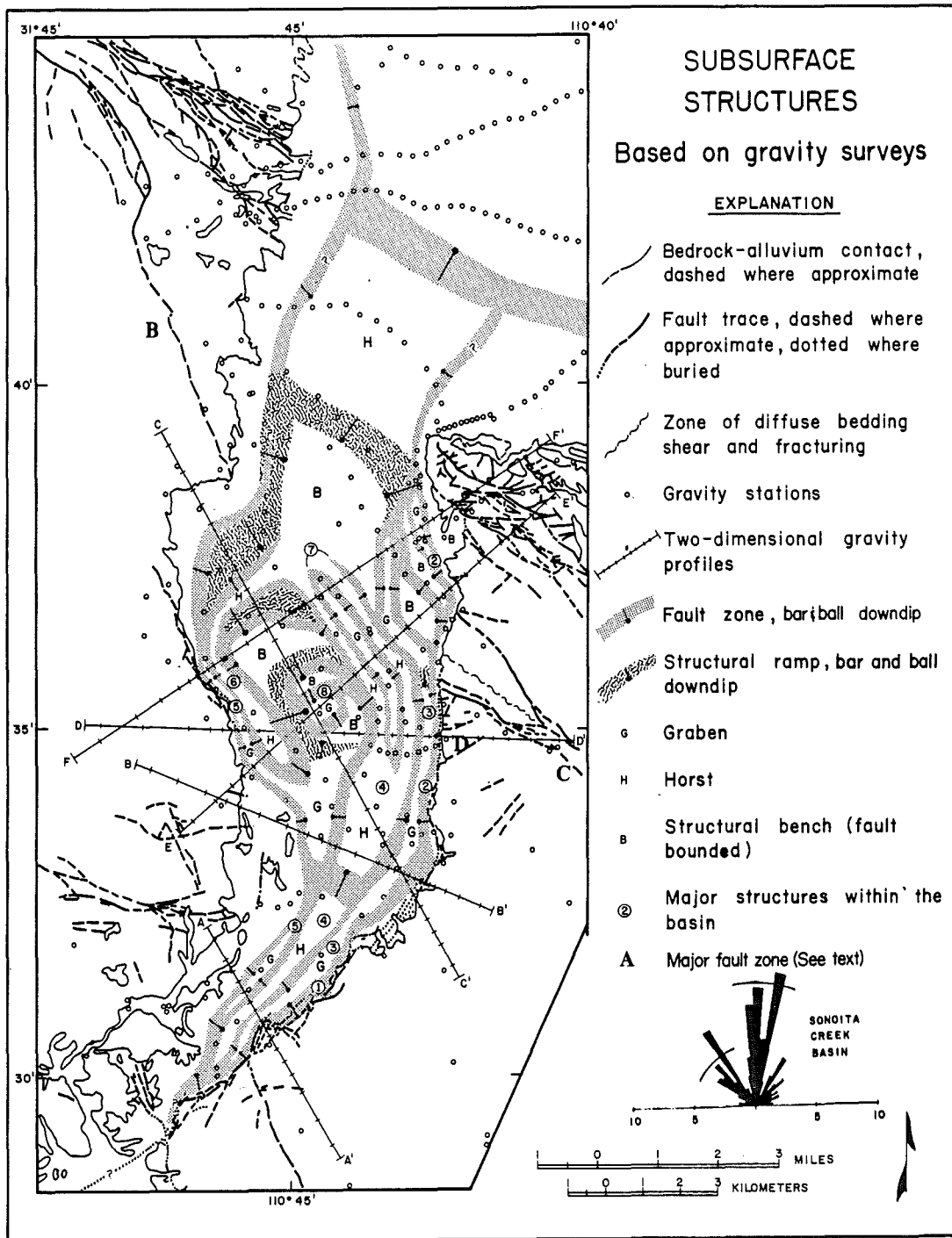


Figure A-2. See next page for explanation

Figure A-2. Interpretative Subsurface Structural Map of the Sonoita Creek Basin study site. -- The interpretations are based on both 2-dimensional modeling of the residual gravity anomaly and surface data. The numbers indicate structural features which both appear in two or more adjacent profiles and are consistent with available gravity and surface data. The letters refer to major surface structures discussed in the text. The Rose diagram represents azimuth orientations of the important interpretative subsurface features of the map.

boundaries), that resemble the segmented southwest border observed in the Hassayampa-basin gravity study. Similar segmented basins and boundary fault zones occur throughout the Basin and Range province of southern Arizona (Menges, 1981; Lysonski, 1980; Oppenheimer and Sumner, 1980).

In the Sonoita Creek basin, one such boundary, the Patagonia fault zone, has been exceptionally well exposed by basin dissection along the southeastern margin of the basin. Detailed mapping along this fault zone reveals a surprisingly complex rupture pattern characterized by multiple, subparallel to branching, downstepping normal fault strands (Fig. A-3). In detail, the overall N. 45 to 50°E. map trace of the Patagonia fault zone is a composite feature comprising numerous individual segments variously oriented between west-northwest and east-northeast directions.

However, the arrangement of the component fault segments is not completely random but exhibits a fairly pronounced and often repetitive linkage pattern between segments of contrasting orientations (represented in simplified form in Fig. A-4). Specifically, a primary set, characterized by either northeast (N. 20-30° E.) or north-south to north-northeast (N. 0-15° E.) oriented trends and 1.5 km average lengths, collectively define 70 percent of the total exposed length of the Patagonia fault zone located to the southwest of Red Rock Canyon (Figs. A-3, A-4). Moving generally northeastward along the zone, the trace of each primary fault segment, as defined above, terminates against a shorter (~0.45 km) fault segment. These secondary segments generally trend east-northeast (N. 60-90° E.) or west-northwest (N. 65-85° W.) and thus are directed transverse to the trend of the composite Patagonia fault boundary. Frequently these secondary segments appear to be localized near certain intersection points where the Patagonia fault zone truncates similarly trending transverse fault zones in the adjoining mountain block (Fig.

STRUCTURAL MAP - PATAGONIA FAULT ZONE

- Contact
- Mixed depositional-growth fault contact, fanglomerate above bedrock (exposed edge of structural ramp)
- Fault zone, bar and ball on downthrown side
Dashed where approximate, dotted where buried (by Quaternary deposits)
- Broad bedrock fault zone with extensive brecciation and alteration
- Zone of concentrated fracturing and minor faulting
- Fold axis (syncline and anticline)
- Axis of basinward bedding rotation
- Bedrock slide block interbedded in basal fanglomerate

Intraformational
Fanglomerate
deformation

Tertiary fanglomerate and
Quaternary pediment-
terrace alluvium

Bedrock

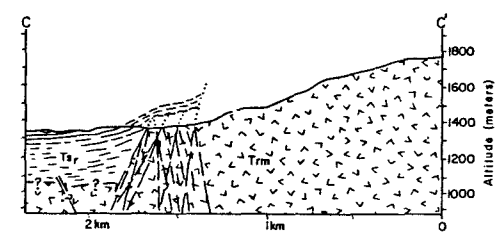
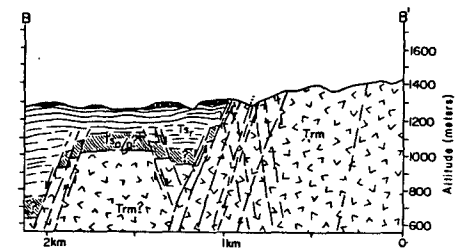
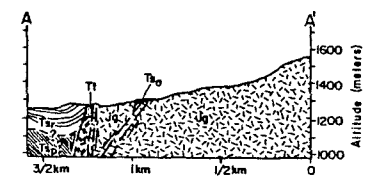
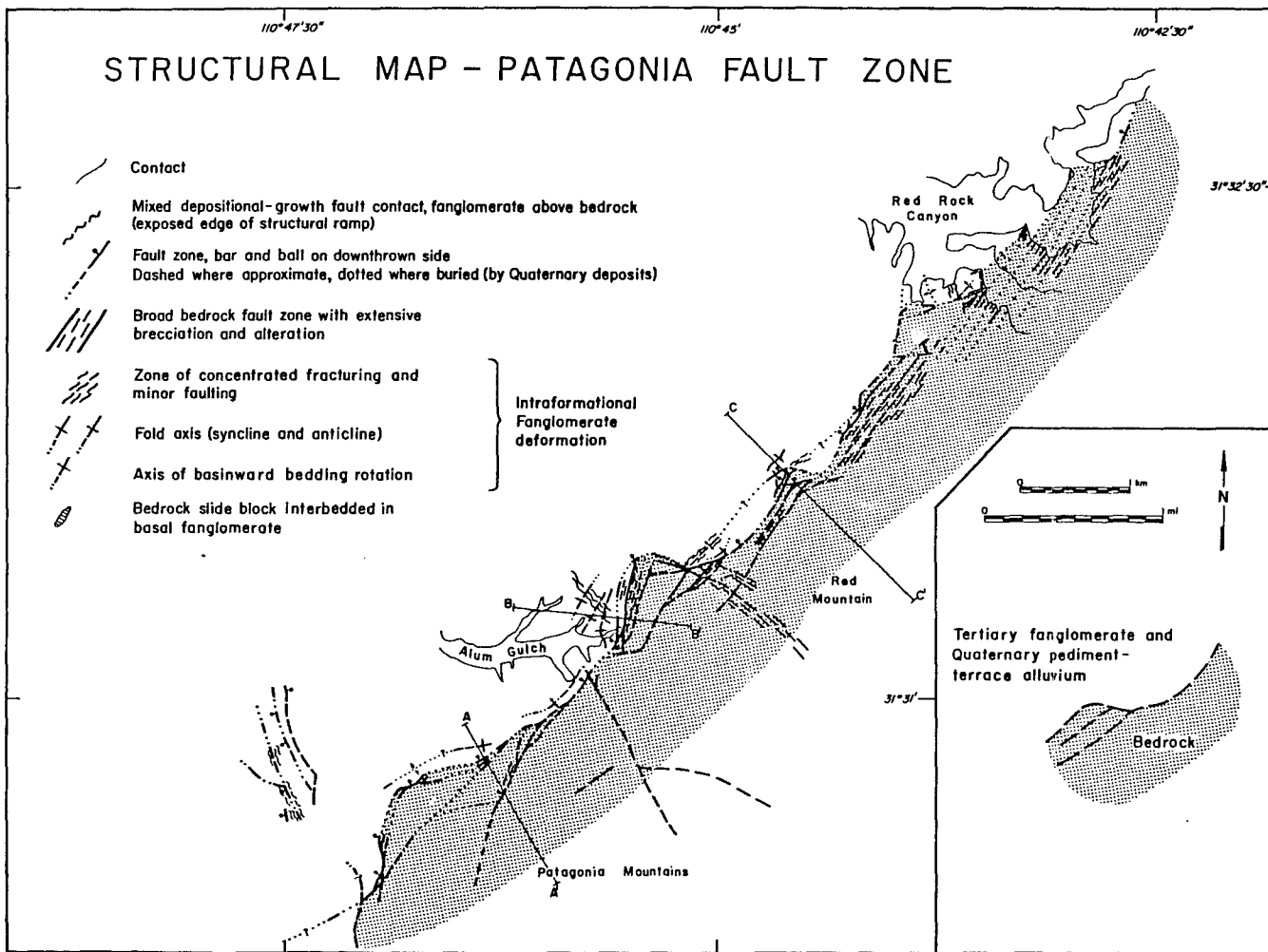


Figure A-3. Structural Map and Cross Sections of the Patagonia Fault Zone.
-- Important structural features are described in the text.
The cross sections are presented at expanded scale (1.5 times map scale) without any vertical exaggeration. Symbols are as follows: (Jg) - Jurassic granite; (Tt) - Tertiary tuff; (Tv) - Paleocene (?) Red Mountain volcanics; (Ts_r) - Red Mountain sediments; (Ts_o) - Older Tertiary sediments; (Ts_o/p(?)) possible occurrence of various Tertiary sediments.

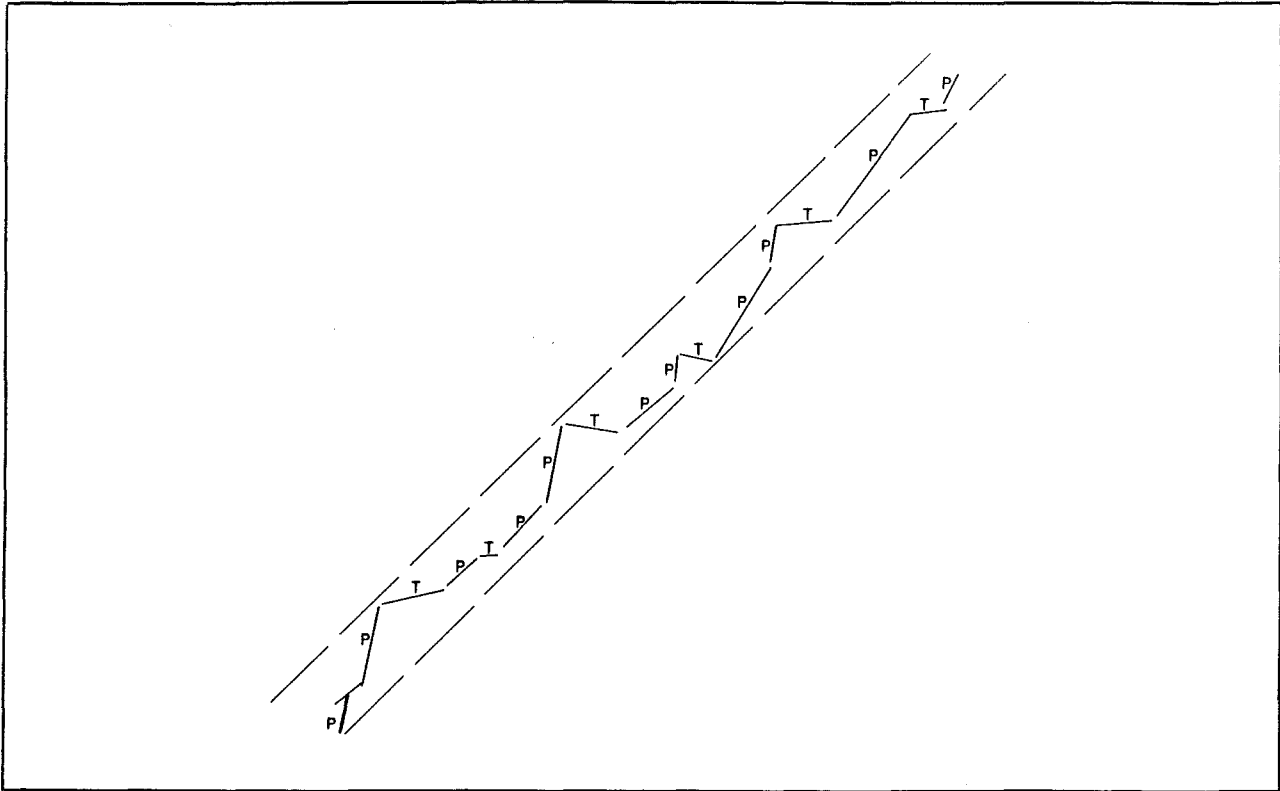


Figure A-4. Schematic and partially idealized diagram of the Patagonia fault zone showing its right-stepping linked; en-echelon segmentation patterns. Both primary (P) and secondary transverse (T) segments are indicated. Refer to text for explanation.

A-3). The boundary of the basin is translated by each transverse segment a short distance to the east and southeast, at which point the boundary again deflects abruptly into another primary north-south to northeast directed fault strand. This segmentation cycle is repeated to varying degrees approximately six to seven times along the exposed length of the Patagonia fault zone (Figs. A-3, A-4). The component segments repeatedly fluctuate about a central axis during each successive cycle, thereby defining the average and dominant northeast trend of the composite Patagonia fault zone boundary.

This segmentation displays a distinct asymmetry in both relative (i.e., proportional) distribution and the structural characteristics of the component sets. First, one fault set dominates over the other in frequency of occurrence, average segment length, cumulative segment lengths, and hence percentage of the composite Patagonia fault zone. Secondly, this primary set of fault segments also incorporates most of the major homothetic fault boundaries along the Patagonia subgraben, as defined earlier (Fig. A-4). The secondary transverse elements in many cases are represented by structural ramps and (or) distributive fault zones with second-order structural expression, relative to the major boundaries. These transverse segments appear to function at least in part as intervening connector or relay links between the larger scale fault boundaries as they are successively displaced asymmetrically to the right (relative to one another) in a pseudo en-echelon pattern that is confined within the general borders of the Patagonia fault zone itself.

Consequently, the overall asymmetry of the segmentation may be described as a right-steeping, linked en-echelon fault system, although slip indicators on all strands indicate mixed oblique to dip-slip displacements (see below) and kinked but continuous segmentation geometry precludes significant lateral slip along the zone. Several other workers have describes similar,

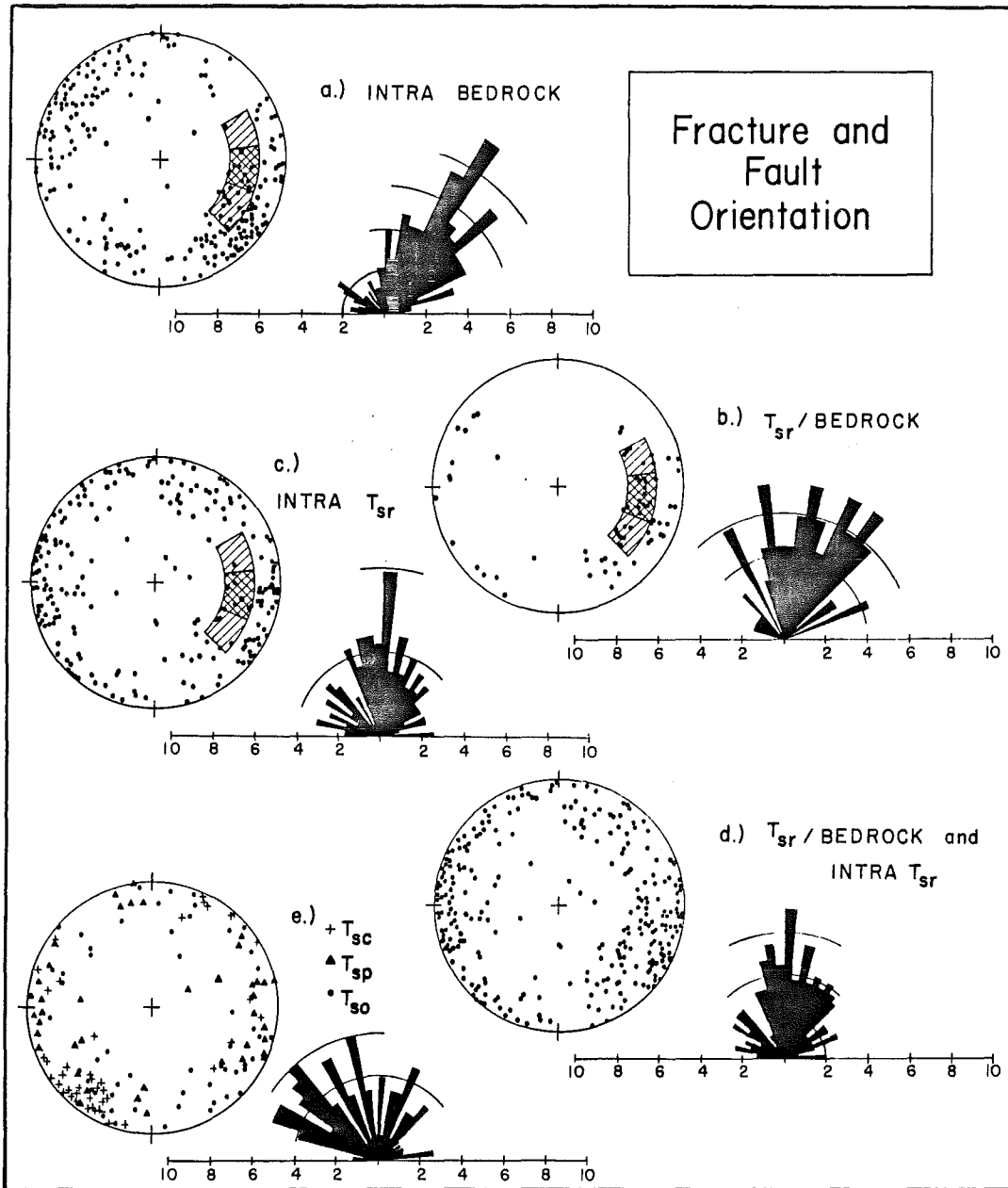


Figure A-5. See next page for explanation

Figure A-5. Orientation Diagram of Individual Faults and Fractures within the Patagonia Fault Zone. -- The display includes both π -axis lower hemisphere stereographic projections and cumulative percentage Rose diagrams of strike azimuth (using 5° class intervals). The data are subdivided according to structural domains which are defined in the text. Hachured areas in plots A-C represent reproductions of the π -axes concentrations observed in plot B.

- A) Intrabedrock domain.
- B) Ts_r /bedrock boundary fault domain.
- C) Intrasediment (Ts_r) domain.
- D) Composite of plots B and C above.
- E) Combination of intrasediment and boundary fault domains in other stratigraphic units.

albeit larger scale, asymmetric linked en-echelon patterns within normal fault boundaries of the central Rio Grand Rift (Ramberg and Smithson, 1975; Woodward and DuChayne, 1975; Ramberg, Cook and Smithson, 1978; Kelley, 1979).

Detailed structural analysis within the Patagonia fault zone provides information regarding the possible kinematic-dynamic significance of fault segmentation geometry. Basically, the structural analysis consisted of orientation studies of outcrop-scale normal faults and extensional fractures collected within three domains of the faults zone (see Menges, 1981, for a complete discussion). These domains are: (a) an intrabedrock domain (structures entirely within internal bedrock portions of the zone, Fig. A-5a); (b) a boundary fault domain (deformation within structural boundaries between bedrock and basin sediments, Fig. A-5b); and (c) an intrasediment domain (structures with several types of basin sediments (Figs. A-5c and e), including one, the Ts_r unit (Fig. A-5c), which was deposited contemporaneous with faulting along the Patagonia fault boundary). The boundary fault and Ts_r intrasediment domains, which contain structures directly correlatable in time to Basin-Range deformation along the Patagonia fault zone, display pronounced north-northwest-, north-, northeast-trending peaks in their strike azimuths (Figs. A-5b and c; combined into one diagram in Fig. A-5d).

Application of Mohr-Coulomb fault mechanics theory to this preferred orientation implies west-southwest to west-northwest (~E-W) extension and extensional stress during Basin-Range deformation along the Patagonia fault zone (Menges, 1981; Menges and others, 1981). This extension direction is oriented oblique to the dominant northeast trend of not only the composite fault trace, but also the component intrabedrock structures (Figs. A-3, A-5a). The intrabedrock domain also contains a distinct group of shallowly plunging slickensides, which although not present in sediment-related domains, closely resemble striae patterns observed on late Cretaceous to early Tertiary faults

exposed in adjacent mountain blocks (Menges, 1981; Davis, 1979). Thus, the present basin-bounding Patagonia fault zone likely represents Basin-Range reactivation of a pre-existing northeast-striking (Laramide(?)) structure. However, comparisons among the fracture and fault orientations of the three structural domains indicate that the sediment-bedrock boundary faults trend more northerly than intrabedrock structures and thus include the preferred orientations of the Ts_r intrasediment domain (Figs. A-5a-c). These relationships suggest selective reactivation within the Patagonia fault zone of those bedrock structures orientated more favorably (north-northwest and north-north east) with respect to east-west extension that was directed oblique to the northeast-trend of the pre-existing fault zone.

Very likely this statistical frequency orientation analysis translates spatially into the observed segmentation pattern, since the primary or dominant fault segments by and large exhibit similar north-northwest to north-northeast orientations. Thus they probably represent some combination of preferential fault reactivation and primary fault rupture, developed in response to the obliquely applied extension and extensional stress. Since these segments trend oblique to the pre-existing fault zone, the primary strands are of necessity repetitively relayed in the direction of the older zone by the secondary transverse segments (Fig. A-6b). The degree and orientation of the resultant segmentation asymmetry (i.e., the linked en-echelon pattern) appears controlled by the orientations of the obliquely applied extensional stress and the reactivated structure relative to one another, as well as the specific configuration of the pre-existing internal fault zone fabric.

Thus, the asymmetric segmentation of the Patagonia fault zone likely represents a quasi-systematic geometric adjustment between several competing variables, which include: (a) complex fault rupture patterns associated with

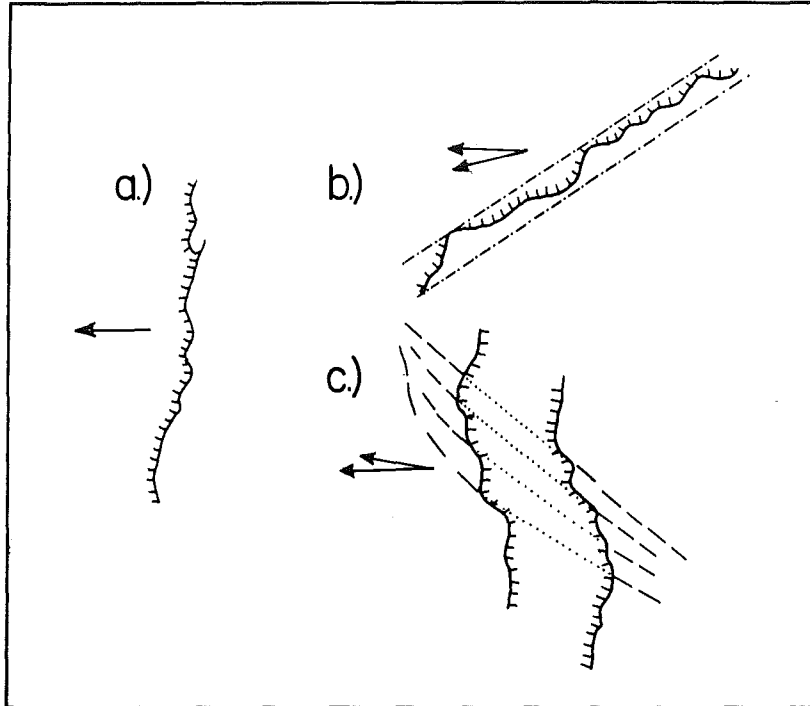


Figure A-6. Schematic Diagram Illustrating Several Normal Fault Segmentation Patterns. -- The arrows indicate average horizontal extension directions, and hachures are on the downthrown side of fault ruptures.

- A) Three-dimensional fault rupture pattern, under general strain conditions, and in isotropic medium (generalized from Fig. 14, Ramberg and others, 1977).
- B) Internal segmentation pattern developed within a complex fault zone reactivated under obliquely-applied extension. The dashed lines represent the approximate cumulative boundary of the older zone, and the heavier lines indicate the actual rupture pattern. (Example: the Patagonia fault zone).
- C) Segmentation pattern created by interference between two intersecting fault zones, as, for example, when one fault zone (solid lines), forming in response to an applied tectonic stress, crossed a pre-existing transversely-oriented fault set (dashed and dotted lines).

general strain in an ideal isotropic medium (Oertel, 1965; Ramberg and others, 1978; Reches, 1978; reproduced in Fig. A-6a); (b) the direction of obliquely applied extension; and (c) selective reactivation of a pre-existing complex fault zone (Fig. A-6b).

A somewhat related segmentation variant appears to occur in the Sonoita Creek basin where fault rupture extends across a zone of intersection with one or more pre-existing fault zones with contrasting orientations. Commonly a composite zigzag rupture pattern emerges, which probably reflects interference between variously reactivated components of the intersecting fault sets, possibly augmented by primary rupture as well (Fig. A-6c). Again, the composite boundary zone may display either symmetric or asymmetric linked en-echelon segmentation across the zone of interference (see above). The degree of asymmetry depends upon both the direction of extension with respect to the orientations of the various fault sets, as well as their relative potential for fault reactivation. Good examples of this interference segmentation process may be observed along the southwest and northeast boundaries of the main Sonoita Creek graben (Fig. A-2).

The gravity signature of the southwestern boundary fault of the northern Hassayampa Plain forms a mirror image of the asymmetric segmentation of the Patagonia fault zone. In the terminology outlined earlier, the Hassayampa boundary fault exhibits left-stepping linked en-echelon asymmetric segmentation. Based upon the structural interpretations presented above, left-stepping asymmetric fault segmentation would be favored if approximately east-west directed extension were obliquely applied to a northwest-trending fault zone formed and (or) reactivated during the Basin-Range disturbance.

REFERENCES

- Davis, G.H., 1979, Laramide folding and faulting in southeastern Arizona: Am. Jour. Sci., v. 279, p. 543-569.
- Kelley, V.C., 1979, Tectonics, middle Rio Grande Rift, New Mexico, in Reicker, R.E. (ed.), Rio Grande Rift tectonics and magmatism, p. 57-70.
- Lysonski, J.C., 1980, The IGSN, Residual Bouguer Gravity anomaly map of Arizona: M.S. Thesis, University of Arizona, Tucson, 74 p.
- Menges, C.M., 1981, The Sonoita Creek Basin: Implications for late Cenozoic tectonic evolution of basin and ranges in southeastern Arizona (M.S. thesis): Tucson, University of Arizona, 239 p.
- Menges, C.M., Mayer, L., and Lynch, D.J., 1981, Tectonic significance of a post-mid-Miocene stress rotation inferred from fault and volcanic vent orientations in the Basin and Range province of southeastern Arizona and northern Sonora (abst.): Geol. Soc. American, Abst. w/Programs, v. 13, no. 2, p. 96.
- Oppenheimer, J.M. and Sumner, J.S., 1980, Depth-to-bedrock map, Basin and Range province, Arizona: Laboratory of Geophysics, University of Arizona, Tucson, scale, 1:1,000,000.
- Ramberg, I.B., Cook, F.A., and Smithson, S.B., 1978, Structure of the Rio Grande rift in southern New Mexico and west Texas based on gravity interpretation: Geol. Soc. American Bull., v. 89, p. 107-123.
- Ramberg, I.B. and Smithson, S.B., 1975, Gridded fault patterns in a late Cenozoic and a Paleozoic continental rift: Geology, v. 3, no. 4, p. 201-205.
- Reches, Z., 1978, Analysis of faulting in three-dimensional strain field: Tectonophysics, v. 47, p. 109-129.
- Woodward, L.A. and DuChayne, H.R., 1975, Geometry of Sierrita fault and its bearing on tectonic development of the Rio Grande Rift, New Mexico: Geology, v. 3, no. 3, p. 114-116.